

# Structure of the Higher Plant Light Harvesting Complex I: In Vivo Characterization and Structural Interdependence of the Lhca Proteins<sup>†</sup>

Frank Klimmek,<sup>\*,‡</sup> Ulrika Ganeteg,<sup>‡</sup> Janne A. Ihalainen,<sup>§</sup> Henny van Roon,<sup>§</sup> Poul E. Jensen,<sup>||</sup> Henrik V. Scheller,<sup>||</sup> Jan P. Dekker,<sup>§</sup> and Stefan Jansson<sup>‡</sup>

Department of Plant Physiology, Umeå Plant Science Centre, SE 90189 Umeå, Sweden, Department of Physics and Astronomy, Biophysics, Free University Amsterdam, De Boelelaan 1081, 1081 HV Amsterdam, Netherlands, and Department of Plant Biology, The Royal Veterinary and Agricultural University, 40 Thorvaldsensvej, DK 1817 Frederiksberg C, Copenhagen, Denmark

Received October 1, 2004; Revised Manuscript Received December 8, 2004

**ABSTRACT:** We have investigated the structure of the higher plant light harvesting complex of photosystem I (LHCI) by analyzing PSI–LHCI particles isolated from a set of *Arabidopsis* plant lines, each lacking a specific Lhca (Lhca1–4) polypeptide. Functional antenna size measurements support the recent finding that there are four Lhca proteins per PSI in the crystal structure [Ben-Shem, A., Frolov, F., and Nelson, N. (2003) *Nature* 426, 630–635]. According to HPLC analyses the number of pigment molecules bound within the LHCI is higher than expected from reconstitution studies or analyses of isolated native LHCI. Comparison of the spectra of the particles from the different lines reveals chlorophyll absorption bands peaking at 696, 688, 665, and 655 nm that are not present in isolated PSI or LHCI. These bands presumably originate from “gap” or “linker” pigments that are cooperatively coordinated by the Lhca and/or PSI proteins, which we have tentatively localized in the PSI–LHCI complex.

In higher plants the primary photochemistry of light-induced charge separation and splitting of water to yield oxygen is performed in the chloroplast thylakoid membrane by the cooperative action of photosystems I (PSI) and II (PSII). The two photosystems share structural similarities, and the chromophores bound to these multiprotein complexes can be divided into distinct groups according to their primary functions. A few pigments participate directly in charge separation (“special pairs”) and secondary electron transfer in the core of the photosystem. These pigments are surrounded by a group of chlorophylls and carotenoids delivering energy to them (“inner antenna”) that are also coordinated by central reaction center proteins. Around the periphery, a number of chlorophyll/carotenoid binding proteins (“outer antenna”) are closely associated with PSI (Lhca1–4) and PSII (Lhcb1–6). Two proteins of this LHC<sup>I</sup> gene family (1–3), Lhcb1 and Lhcb2, form a mobile trimeric complex (LHCII) that can be associated with either photosystem, allowing the relative antenna sizes to be adjusted and the excitation pressure to be balanced under varying light

conditions, via a mechanism known as “state transition” (for a review see ref 4).

Single particle electron microscopy and crystal diffraction pattern studies have provided clear information about the position of individual subunits in LHCII (5, 6) and PSII (7, 8) as well as the molecular organization of the PSII/LHCII macrocomplex (9, 10), both in cyanobacteria and higher plants. In comparison, the light-harvesting antenna of higher plant PSI (LHCI) has not been as well characterized. The first structures published for PSI have been obtained from cyanobacteria (11–14), which do not contain LHCI-like antenna. However, ring structures around cyanobacterial trimeric PSI complexes have been reported to be induced under iron deficiency (15–17). These rings are composed of multimeric copies of the IsiA protein, a homologue of the PSII reaction center protein CP43, and have been shown to serve as functional antennae for PSI (18, 19). Green algae contain a variety of Lhca-like proteins (20, 21), but the recently published low-resolution PSI–LHCI structure of *Chlamydomonas reinhardtii* (22, 23) seems to contain considerably more Lhca-like proteins than its counterpart in higher plants (24). Various PSI–LHCI particles have been prepared from green plants by ultracentrifugation after solubilizing thylakoid membranes with different detergents (25–28), and four types of LHCI proteins (Lhca1, Lhca2, Lhca3, and Lhca4) have been found to be regularly associated with PSI (26, 29, 30). These proteins have been assumed to be present in a stoichiometric ratio close to 1:1:1:1 (2, 31), but the ratio may vary under certain conditions, due either to mutations or to changes in growth conditions (32–35). In addition, a novel type of Lhca protein, Lhca5, has recently been found to associate with PSI (36, 37).

<sup>†</sup> This work was supported by grants from the Swedish Research Council for Environment, Agricultural Sciences and Spatial Planning and the European Community’s Human Potential Program under Contract HPRN-CT-2002-00248 (PSICO).

\* To whom correspondence should be addressed. Phone: 46-90-786 57 41. Fax: 46-90-786 66 76. E-mail: frank.klimmek@plantphys.umu.se.

<sup>‡</sup> Umeå Plant Science Centre.

<sup>§</sup> Free University Amsterdam.

<sup>||</sup> The Royal Veterinary and Agricultural University.

<sup>1</sup> Abbreviations: Chl, chlorophyll; LHC, light harvesting complex; Lhca and Lhcb, apoprotein of a light harvesting complex of photosystem I and II, respectively; PS, photosystem; P700, reaction center of photosystem I; RP-HPLC, reversed-phase high-pressure liquid chromatography; wt, wild type.

In higher plants, LHCI has peculiar fluorescence characteristics with red-shifted emission spectra due to a few chlorophyll molecules, so-called red chlorophylls, with an energy level lower than that of the PSI reaction center. These red chlorophylls are capable of uphill excitation energy transfer to the reaction center, and although their presence slows down trapping by charge separation (38), the efficiency of trapping is not markedly affected (39). They were first believed to be confined to the so-called LHCI-730 complex, consisting of an Lhca1/Lhca4 heterodimer, as preparations of Lhca2 and Lhca3 (LHCI-680) exhibited more blue-shifted emission peaks (29, 40), until it was found that Lhca2 and Lhca3 also bind red chlorophylls (35, 41). Lhca2 and Lhca3 might form heterodimers *in vivo* (24, 42, 43), but it is not known for certain if they can also form homodimers. Recently, the evolution of long-wavelength fluorescence in LHCI was shown to be predominantly associated with an asparagine-bound chlorophyll on site a5 (44, 45) in Lhca3 and Lhca4. In Lhca1, Lhca2, and Lhca5, as well as in the Lhcb-type proteins, this binding site contains a histidine, and consequently, reconstituted monomers of these proteins do not show long-wavelength fluorescence (45, 46).

Single particle electron microscopy studies have indicated that the entire LHCI binds to one side of the PSI complex (47). On the other side of the complex, PSI-H forms a docking site for mobile LHCII (Lhcb1/Lhcb2) trimers (48), while other small PSI subunits, such as PSI-L and PSI-O, may also be involved in LHCII-PSI interactions (49, 50). The amount of Lhca proteins per PSI within the LHCI has been estimated to range between six and eight (26, 30, 43), but according to the recent model obtained from crystallography at 4.4 Å resolution (24), only four Lhca proteins assemble with one PSI reaction center. Since the different Lhca types cannot be distinguished at this resolution, their positions in the crystal structure have been based on previously obtained data from cross-linking studies (42) and the protein composition of mutants missing either PSI reaction center proteins (for a review see ref 51) or Lhca proteins (32, 35).

A total of 167 chlorophylls have been localized in the PSI structure (24), 56 of which seem to be coordinated by the four Lhca proteins of LHCI. The implied ratio of 11–14 chlorophylls per Lhca polypeptide is higher than the ratio found in a number of *in vitro* reconstitution studies, where 6–10 chlorophylls have been reported to be bound by each Lhca protein (43, 44, 52, 53). This indicates that pigments either loosely associate with the individual polypeptides or that pigments located at the interfaces between the proteins need more than one protein for stable association. In either case, their weak binding complicates biochemical studies, since the individual proteins are difficult, or perhaps impossible, to purify in their native state, and *in vitro* reconstitution studies are unlikely to reflect the *in vivo* situation. By applying reverse genetic techniques such as antisense inhibition and T-DNA knock-out mutagenesis, plants lacking individual gene products can be produced. Since none of the LHC proteins are essential for growth under laboratory conditions, the plants can be grown and subjected to various analyses to pinpoint the characteristics of the individual proteins. We have previously produced a full set of *Arabidopsis* plants in which each of the four *Lhca* genes are individually repressed or knocked out and have characterized

them in terms of thylakoid polypeptide composition and low-temperature chlorophyll fluorescence emission of intact leaves and monitored their fitness in terms of seed production under natural conditions (33, 35, 54). In this contribution, we report experiments in which we subjected the plant collection to an array of biochemical and spectroscopic analyses in order to learn more about the structure of LHCI and its pigment-binding properties.

## MATERIALS AND METHODS

**Plant Material.** The wild-type (WT; ecotypes Colombia and C24), antisense ( $\Delta$ Lhca2-a4), and T-DNA knock-out lines ( $\Delta$ Lhca1) of *Arabidopsis thaliana* used in this study have been described earlier (33, 35, 54). It has been previously shown that the antisense lines do not accumulate the respective targeted proteins, and their phenotypes in terms of LHC protein composition are consistent in several individual antisense lines resulting from different transformation events. During the course of this work a T-DNA knock-out line for Lhca4 (SALK-127744, 55) that yields undetectable amounts of Lhca4 was isolated. This plant line had the same Lhca polypeptide content and showed the same growth phenotype as the antisense Lhca4 plants. Therefore, we do not distinguish between these lines in this report, and we did not repeat all analyses for both lines of Lhca4-deficient plants. For Lhca1, we have used an *Arabidopsis* line with a T-DNA insertion in the promoter region of *Lhca1* that causes a decrease in Lhca1 content to 2–5% of wild-type levels. All plants were grown on soil/perlite in a growth chamber under fluorescent lamps with a photon flux density of 150  $\mu\text{mol m}^{-2} \text{s}^{-1}$ , a light/dark regime of 6/18 h, a temperature regime of 23/18 °C, and 75% relative humidity.

**Preparation and Immunoblotting of Thylakoids and PSI.** Thylakoids were prepared from 6–7-week-old dark-adapted plants (56), and PSI particles were isolated by solubilizing the thylakoids with dodecyl  $\beta$ -D-maltoside (Sigma) with subsequent ultracentrifugation on sucrose gradients (28). Samples were concentrated to a chlorophyll content of 0.8–2 mg/mL in centrifugal concentrators (Centricons YM-10, Millipore), and the chlorophyll content was determined photometrically (36). SDS-PAGE and immunoblotting were performed as previously described (35).

**Pigment Analysis.** Following the method in ref 57, pigments were extracted with 80% acetone, centrifuged, and loaded on an RP-HPLC column (Lichrosorb C18, 10  $\mu\text{m}$ , 250  $\times$  4.6 mm), which was equilibrated in buffer A [85% acetonitrile, 13.5% methanol, 1.5% 0.2 M Tris-HCl (pH 8.0)]. After 15 min of isocratic flow at 1 mL/min the neoxanthin, violaxanthin, and lutein were eluted from the column. After a linear gradient of 3 min to buffer B (83.3% methanol, 16.7% *n*-hexane) and an isocratic run for 40 min with buffer B, the chlorophylls and carotenes were eluted. The column was then rinsed with methanol for 10 min and again equilibrated with buffer A. The HPLC system was equipped with a diode array optical absorption spectrophotometer, which allowed peaks in the chromatogram to be identified by their absorption spectra.

**Antenna Size Measurements.** Isolated PSI particles were subjected to saturating light pulses of actinic light, and the changes in absorbance of the oxidized P700 at 810 nm were determined as described (58), except that 22.5  $\mu\text{g}$  of total

chlorophyll was used in a volume of 750  $\mu\text{L}$ . Averaged absorption curves were recorded for 1000 ms for series of eight pulses of 1 s with 20 s intervals at two different intensities (40.6 and 76.6  $\mu\text{mol}$  of photons  $\text{m}^{-2} \text{s}^{-1}$ ) of actinic light for two independently prepared samples with three to six replicates. The absorption curves were fitted with single-exponential functions, and relative antenna sizes (percent of wild type) were calculated from the halftimes ( $t_{1/2}$ ) with the assumption that all chlorophylls functionally connected to a reaction center contribute equally to P700 oxidation in the monitored millisecond time scale.

**Absorbance Spectroscopy.** The samples were diluted in 20 mM Bis-Tris (pH 6.5), 20 mM NaCl, 0.06%  $\beta$ -DM, and 66% (v/v) glycerol to an optical density of about 0.6  $\text{cm}^{-1}$  at 680 nm and placed in acrylic cuvettes with a 1 cm optical path length. The samples were cooled to 5 K in a helium bath cryostat (Utreks, Ukraine), and absorption spectra were measured using a spectrometer, built in-house, with an optical bandwidth of about 1.3 nm. The resulting absorption spectra were first normalized to the same total chlorophyll content. The spectra were then multiplied by estimated chlorophyll/RC factors of wild type and mutants, as appropriate, and wild-type minus  $\Delta\text{Lhca}$  difference absorption spectra were constructed.

**Emission Spectroscopy.** The samples were diluted to an optical density of about 0.1  $\text{cm}^{-1}$  at 680 nm and cooled to 5 K as described above. Fluorescence emission spectra were then measured with a  $1/2$  m imaging spectrograph and a CCD camera (Chromex Chromcam I). The spectral resolution was about 0.5 nm. For broad-band excitation a tungsten halogen lamp (Oriol) was used with band-pass filters transmitting at 420 and 475 nm (bandwidth of 20 nm). The obtained emission spectra were corrected for the wavelength-dependent sensitivity of the detection system.

## RESULTS

The depletion of individual Lhca proteins affects the association of the other main Lhca-type polypeptides (Lhca1–4) to the PSI core, as shown by western blot analysis of thylakoids (Figure 1A) and the PSI–LHCI preparations (Figure 1B) used in this study. In addition, the level of Lhca5 content is decreased in plants lacking Lhca2 and elevated in the plants depleted in Lhca1 and Lhca4. Preparations from the latter line yielded PSI–LHCI particles that were virtually devoid of all Lhca proteins, except Lhca5. But as this protein could not be detected either in Coomassie- or silver-stained gels (data not shown), the total protein amount has to be judged as rather low despite a strong antibody signal. The Lhca protein content analysis of the PSI–LHCI particles confirms previous reported data on this lines (35, 36, 54).

**Antenna Size and Pigment Composition of Lhca-Deficient PSI Particles.** We have determined the functional antenna sizes and pigment stoichiometries of the PSI particles described in Figure 1B. On the basis of the measured oxidation kinetics of P700, which is proportional to the total amount of chlorophyll transferring energy to P700, the relative antenna sizes of all Lhca-deficient plants were significantly reduced (Table 1). This reduction was highest for  $\Delta\text{Lhca4}$  (32%) and  $\Delta\text{Lhca2}$  plants (25%), while the antennas of  $\Delta\text{Lhca1}$  (17%) and  $\Delta\text{Lhca3}$  plants (19%) were less strongly, but still clearly, affected. Measurements at two

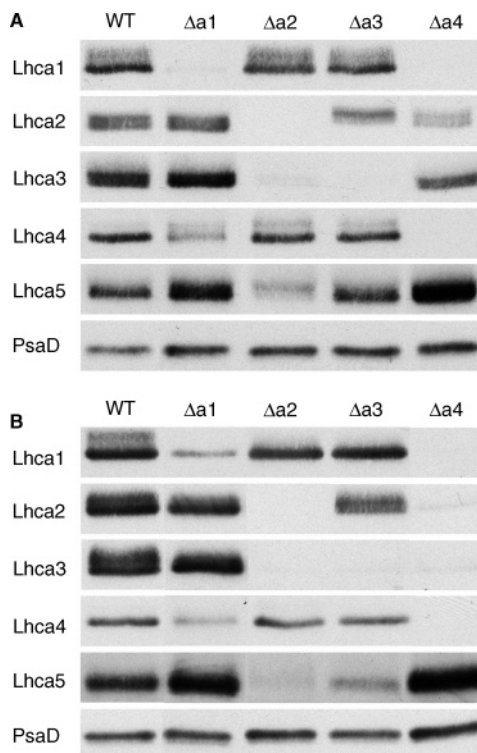


FIGURE 1: Effect of LHCI depletion on Lhca protein content. The Lhca protein content of (A) thylakoids and (B) PSI preparations (2  $\mu\text{g}$  of Chl per lane) from wild-type (WT) and  $\Delta\text{Lhca1}$ –4 ( $\Delta\text{Lhca1}$ –4) plants was analyzed using immunoblotting.

different light intensities gave consistent data. However, immunoblotting detected a small genotype-specific LHCII content in all PSI preparations (data not shown) that was slightly higher for preparations from the  $\Delta\text{Lhca2}$  and  $\Delta\text{Lhca4}$  plants, which also showed the highest reductions in PSI antenna size. We therefore used the neoxanthin levels determined by HPLC analyses (data not shown) to calculate the LHCII contents on the basis of the pigment-binding pattern of LHCII (6). From the resulting data, we estimated one LHCII trimer to be associated per 12–14 PSI in the wt,  $\Delta\text{Lhca1}$ , and  $\Delta\text{Lhca3}$  lines but the LHCII to PSI ratios to be higher (one LHCII trimer per 11 and 8 PSI, respectively) in  $\Delta\text{Lhca2}$  and  $\Delta\text{Lhca4}$  preparations. Since the PSI–LHCI complex does not contain neoxanthin in vivo, the relative PSI antenna sizes were recalculated by subtracting the LHCII contribution. On the basis of the number of 167 chlorophylls resolved in the PSI–LHCI structure (24), absolute antenna sizes (Chl/P700) can now be calculated for the PSI–LHCI complexes prepared from the Lhca-deficient plants (Table 1). It is interesting to note that the preparations from the  $\Delta\text{Lhca4}$  plants still contain about 12 chlorophylls that must be located on Lhca proteins, since the PSI core only accounts for 101 chlorophylls. This indicates that one Lhca-type protein is present per PSI in these samples. In some cases the putative protein may be Lhca5, but the findings may also be explained by the presence of residual amounts of Lhca2 and Lhca3 in this preparation.

The corrected absolute antenna sizes (Table 1) have been used to normalize the amounts of Chl *b*,  $\beta$ -carotene, and two xanthophylls (lutein and violaxanthin) of the PSI preparations determined by HPLC (Table 2). As expected, the loss of light harvesting proteins clearly affects the amounts of chlorophyll *b* and xanthophyll, while the levels of  $\beta$ -carotene

Table 1: Antenna Sizes for PSI–LHCI Complexes<sup>a</sup>

light ( $\mu\text{E}$ )		WT	$\Delta\text{Lhca1}$	$\Delta\text{Lhca2}$	$\Delta\text{Lhca3}$	$\Delta\text{Lhca4}$
40.6	$t_{1/2}$ (ms)	70.4 $\pm$ 0.9	84.5 $\pm$ 1.3	92.0 $\pm$ 1.7	84.7 $\pm$ 2.1	102.5 $\pm$ 1.8
	rel (%)	100.0 $\pm$ 1.3	83.2 $\pm$ 1.8	76.5 $\pm$ 2.4	83.1 $\pm$ 3.0	68.4 $\pm$ 2.6
76.7	$t_{1/2}$ (ms)	37.5 $\pm$ 0.8	44.7 $\pm$ 1.7	50.4 $\pm$ 1.4	47.1 $\pm$ 1.6	57.1 $\pm$ 1.6
	rel (%)	100.0 $\pm$ 2.0	83.4 $\pm$ 4.5	74.3 $\pm$ 3.7	79.7 $\pm$ 4.2	70.5 $\pm$ 4.1
mean	rel (%)	100.0 $\pm$ 1.6	83.3 $\pm$ 3.2	75.4 $\pm$ 3.0	81.4 $\pm$ 3.6	69.4 $\pm$ 3.3
minus LHCII content		100.0	83.0	74.4	81.0	67.6
total Chl/P700		167.0	138.7	124.2	135.3	113.0

<sup>a</sup> P700 oxidation kinetics for PSI–LHCI complexes prepared from wild-type (WT) and Lhca-deficient *Arabidopsis* lines ( $\Delta\text{Lhca1}$ – $\Delta\text{Lhca4}$ ); values for  $t_{1/2}$  (ms) and relative antenna sizes (%) compared to the wild type are means  $\pm$  standard errors of four to nine measurements on two independent preparations; total numbers of  $n$  Chl  $a + b$  per P700 have been calculated after subtracting LHCII Chl content in the sample (see text).

Table 2: Pigment Composition of PSI–LHCI Complexes<sup>a</sup>

	WT	$\Delta\text{Lhca1}$	$\Delta\text{Lhca2}$	$\Delta\text{Lhca3}$	$\Delta\text{Lhca4}$
Chl $a + b$	167.0	138.7	124.2	135.3	113.0
Chl $a/b$	10.6	13.2	14.4	15.4	32.1
Chl $a$	152.6	128.9	116.2	127.1	109.5
Chl $b$	14.4 $\pm$ 0.8	9.8 $\pm$ 0.1	8.1 $\pm$ 0.1	8.2	3.4 $\pm$ 0.1
$\beta$ -carotene	27.2 $\pm$ 0.1	24.3 $\pm$ 0.6	21.7 $\pm$ 0.3	22.7	21.5 $\pm$ 0.1
lutein	9.8 $\pm$ 0.1	6.4 $\pm$ 0.1	4.4 $\pm$ 0.1	5.4	1.8 $\pm$ 0.1
violaxanthin	5.8 $\pm$ 0.1	2.8 $\pm$ 0.4	2.9 $\pm$ 0.1	2.6	1.1 $\pm$ 0.2

<sup>a</sup> HPLC pigment analysis of isolated PSI–LHCI complexes prepared from wild-type (WT) and Lhca-deficient *Arabidopsis* lines ( $\Delta\text{Lhca1}$ – $\Delta\text{Lhca4}$ ). Amounts of pigments associated with LHCII present in the sample were calculated from the determined neoxanthin content using the ratios given in ref 6 and subtracted from the total pigments. Results ( $\pm$  standard error) are averaged from two independent measurements (except for  $\Delta\text{Lhca3}$ ) and normalized to the total number of  $n$  Chl  $a + b$  per P700 calculated according to Table 1 (see text).

are less affected. The analysis of  $\Delta\text{Lhca2}$  and  $\Delta\text{Lhca4}$  PSI particles indicates that two to six  $\beta$ -carotenes are lost in these plants and are thus most likely coordinated by LHCI. Therefore, the number of 25–27  $\beta$ -carotenes per PSI–LHCI can be compared with the number of 22 assigned in the crystal structure of cyanobacterial PSI (14). Our finding of nine to ten luteins and five to six violaxanthins in a wild-type LHCI is in agreement with previous data from native and reconstituted LHCI complexes (43, 59). Due to the mutual dependencies of the Lhca proteins regarding their binding to the PSI core, clear assignment of bound pigments to individual Lhca proteins is not feasible, but it can be assumed that each of the four Lhca proteins assigned in the structure binds on average 12–14 chlorophylls and 2–3 luteins, as well as 1–1.5 violaxanthins and  $\beta$ -carotenes. These figures differ from the reported numbers of pigments coordinated by reconstituted Lhca proteins, with total numbers (per Lhca protein) of 6–10 chlorophylls, 1.1–1.7 luteins, 0.5–0.8 violaxanthins, 0.2–0.45  $\beta$ -carotenes, and trace amounts of neoxanthin (43, 44, 52, 53, 59–61). It is likely that some of the pigments coordinated in native complexes (especially those located in the interaction sites between the Lhca proteins or between LHCI and the core antenna) may not be incorporated under reconstitution conditions.

**Spectroscopic Properties of LHCI in PSI–LHCI Particles.** As reconstituted systems do not contain all of the pigments bound by the complexes in vivo, we subjected isolated PSI particles from the set of *Arabidopsis* lines to a detailed spectroscopic analysis to connect certain chlorophyll spectral forms to individual Lhca polypeptides. Figure 2 shows the 4 K absorption spectra of the particles prepared from the different lines. The spectra were normalized to the integrated absorption between 620 and 730 nm. It is immediately clear from the spectra that in most cases the absorption bands of red chlorophylls (absorbing at wavelengths longer than 700

nm) and chlorophyll  $b$  (peaking around 650 nm) are diminished, as anticipated since LHCI has higher contents of chlorophyll  $b$  and red chlorophylls than the PSI core complex. The differences were most pronounced for the  $\Delta\text{Lhca4}$  and least pronounced for the  $\Delta\text{Lhca1}$  plants, in accordance with the finding that the  $\Delta\text{Lhca4}$  and  $\Delta\text{Lhca1}$  plants have the highest and lowest LHCI contents, respectively.

We calculated difference spectra (of particles from wild-type plants minus particles from  $\Delta\text{Lhca}$  plants) after normalizing the spectra to the estimated pigment stoichiometries (Table 2; see also Materials and Methods). These spectra (Figure 3) mainly reflect absorption properties of the missing pigments, associated with the corresponding Lhca mutation. Then, absorption properties of pigments between the missing Lhca proteins and the PSI core or between neighboring Lhca proteins can be determined in some extent. A comparison of these difference spectra and spectra of isolated LHCI dimers (41) shows that the difference spectra have clear absorption bands peaking at 688 and 696 nm and shoulders at about 665 nm that are not present in isolated LHCI dimers. Since most linker chlorophylls are probably not present in the spectrum of the isolated LHCI dimers, it is likely that some of the linker chlorophylls absorb preferentially at 665, 688, and 696 nm. The 696 nm band has approximately equal intensity in all spectra, but the 688 nm bands are more pronounced in the spectra dominated by Lhca2 and Lhca3, indicating pigments responsible for 688 nm absorption bands to be in the vicinity of Lhca2 and/or Lhca3. The lack of absorption at 674 nm in the spectra dominated by the Lhca2 or Lhca3 proteins is in line with observations from reconstituted Lhca proteins, where Lhca3 does not show any absorption at 674 nm and the absorption maximum of Lhca4 at 5 K is found to be at 674 nm (43; R. Croce and J. Ihalainen, unpublished results).

In the chlorophyll  $b$  absorption region, there is increased absorption at 643 nm in the spectra dominated by Lhca1

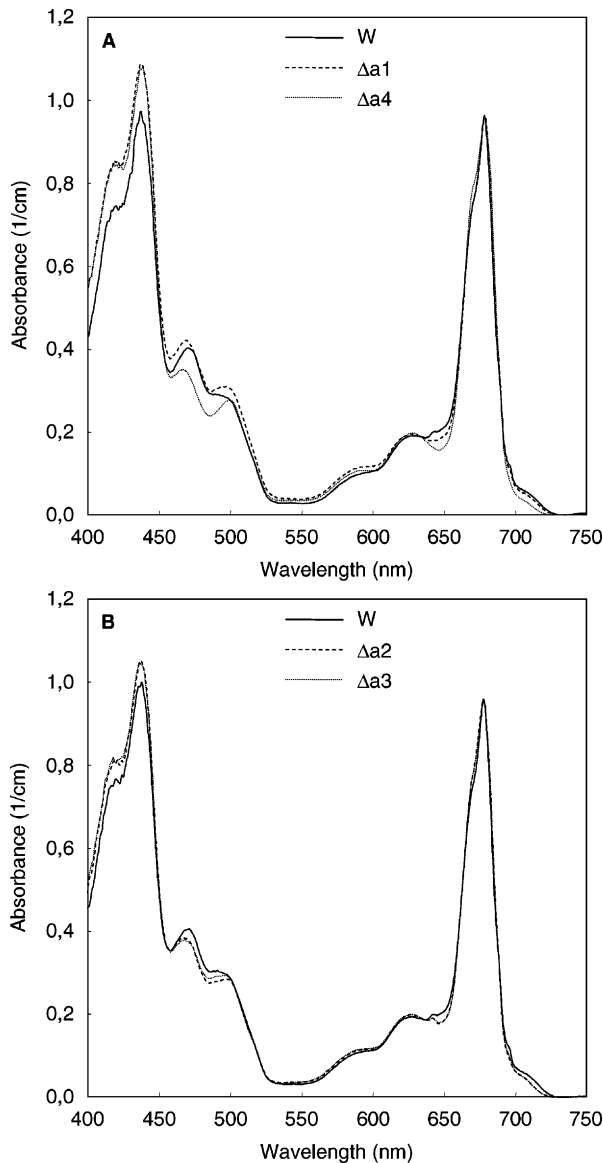


FIGURE 2: Absorption spectra at 4 K of wild-type (WT) PSI together with (A)  $\Delta$ Lhca1 ( $\Delta$ a1) and  $\Delta$ Lhca4 ( $\Delta$ a4) spectra and (B)  $\Delta$ Lhca2 ( $\Delta$ a2) and  $\Delta$ Lhca3 ( $\Delta$ a3) spectra. The spectra are normalized to the same chlorophyll *a* oscillation strength at the  $Q_y$  region.

and Lhca4 and at 650 and 655 nm in the spectra dominated by Lhca2 and Lhca3. This is consistent with absorption spectra of reconstituted Lhca1/4 proteins, which have 643 nm chlorophyll *b* states (43; 52; J. Ihalainen and R. Croce, unpublished results), and partially consistent with absorption spectra of reconstituted Lhca2 and Lhca3 proteins (which have 650 nm chlorophyll *b* states but no clear 655 nm states). These findings suggest that the 655 nm absorption band arises from one or more linker molecules in the vicinity of Lhca2 and/or Lhca3 and that a small proportion of the linker molecules are chlorophyll *b*.

In the red-most absorption region, the spectra dominated by Lhca2 and Lhca3 show a slight red shift compared to those dominated by Lhca1 and Lhca4. The spectra dominated by Lhca2 and Lhca3 peak at 712 nm, which is further to the red than the spectrum of the isolated dimers and considerably further to the red than the spectrum of reconstituted Lhca3 (53; R. Croce and J. Ihalainen, unpublished results). Because the spectra shown here reflect the absorption of Lhca2 and

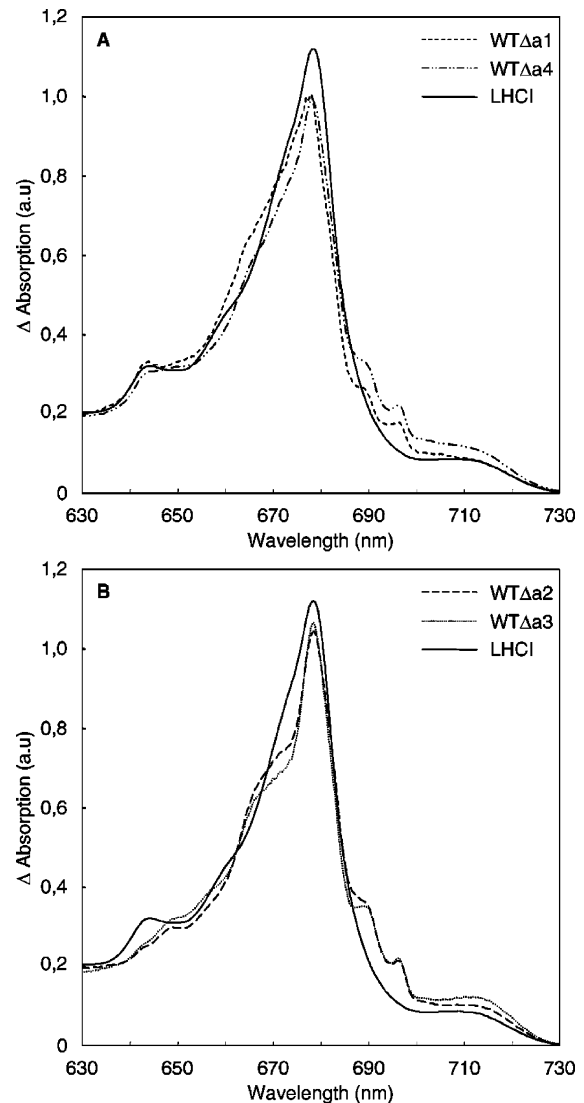


FIGURE 3:  $Q_y$ -region absorption difference spectra at 4 K of wild type minus (A)  $\Delta$ Lhca1/ $\Delta$ Lhca4 (WT $\Delta$ a1, WT $\Delta$ a4) and (B)  $\Delta$ Lhca2/ $\Delta$ Lhca3 (WT $\Delta$ a2, WT $\Delta$ a3) spectra. For details on the construction of the difference spectra see Materials and Methods and Tables 1 and 2. For comparison, the absorption spectra of a native LHCI preparation (41) is shown. All spectra are normalized to the same chlorophyll *a* oscillation strength in the  $Q_y$  region.

Lhca3 within the native PSI–LHCI complex, the binding of these complexes to the PSI core complex probably causes a red shift of the absorption spectra of the red chlorophylls. This red shift is probably caused by excitonic interactions between neighboring chlorophylls within the Lhca3 or Lhca4 (45, 62) and a slight change in conformation of the protein, which very slightly diminishes the distance between the interacting chlorophylls.

We also recorded 4 K fluorescence emission spectra after excitation at 420 nm of the different preparations. The red emission maxima are located at about 734 nm for wild type, 732 nm for  $\Delta$ Lhca1, 724 nm for  $\Delta$ Lhca2, 727 nm for  $\Delta$ Lhca3, and 720 nm for  $\Delta$ Lhca4 PSI preparations after excitation at 420 nm (Figure 4A). The blue shift of the emission spectra of the particles prepared from  $\Delta$ Lhca2 and  $\Delta$ Lhca3 lines is remarkable, because the LHCI protein with the red-most fluorescence spectrum (Lhca4) is still present in PSI preparations from both  $\Delta$ Lhca2 and  $\Delta$ Lhca3 plants, albeit in lower quantities. We note that in vitro reconstituted

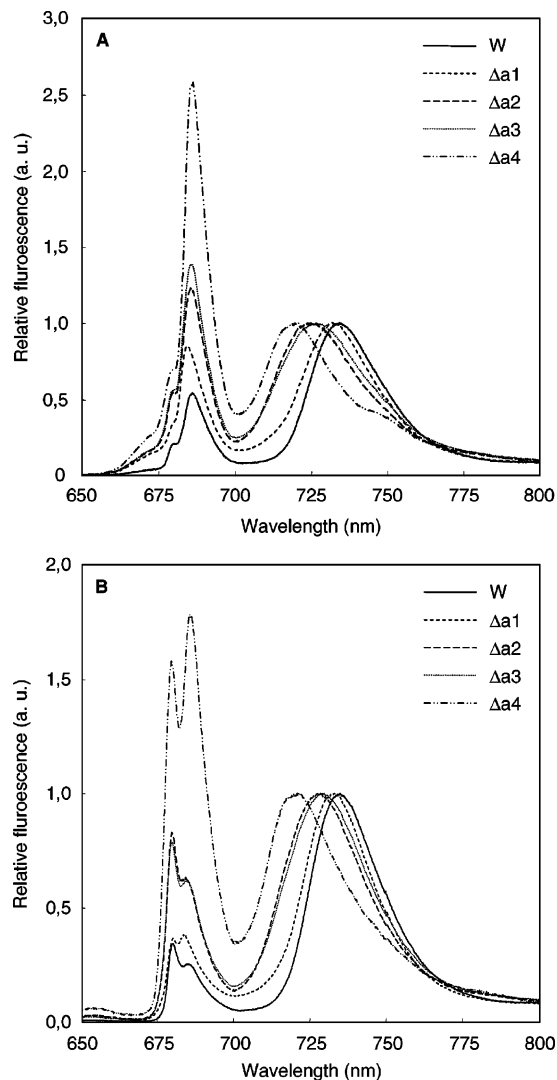


FIGURE 4: Fluorescence emission spectra at 4 K of wild type (WT) and  $\Delta$ Lhca1–4 ( $\Delta$ a1–4) PSI preparations, normalized to their red emission maxima. (A) Excitation at 420 nm. The red emission maxima of the spectra are at about 734 nm for WT, 732 nm for  $\Delta$ Lhca1, 724 nm for  $\Delta$ Lhca2, 727 nm for  $\Delta$ Lhca3, and 720 nm for  $\Delta$ Lhca4. (B) Excitation at 475 nm. The red emission maxima of the spectra are at about 734 nm for WT, 732 nm for  $\Delta$ Lhca1, 728 nm for  $\Delta$ Lhca2, 729 nm for  $\Delta$ Lhca3, and 720 nm for  $\Delta$ Lhca4.

Lhca4 and Lhca3 emit maximally at 730–732 nm (59) and 725 nm (53), respectively, while the isolated PSI core complex emits at around 720 nm at 5 K (63; J. Ihalainen and R. Croce, unpublished results). The blue shift of the  $\Delta$ Lhca2 and  $\Delta$ Lhca3 emissions can be explained by the loss of the 712 nm-absorbing chlorophyll species and by assuming that excitation energy absorbed by pigments in the core antenna is not transferred efficiently to the red chlorophylls in the remaining Lhca proteins, and therefore more is transferred to the red pigments of the PSI core, the emission of which then becomes more prominent. The increased contribution of PSI core emission to the total emission in the  $\Delta$ Lhca2 and  $\Delta$ Lhca3 lines is confirmed by the finding that upon 475 nm excitation the red-most bands of the  $\Delta$ Lhca2 and  $\Delta$ Lhca3 PSI particles are red shifted by 2–3 nm (Figure 4B) compared to 420 nm excitation, which can be explained by the higher excitation rate of the remaining Lhca proteins. In the case of wild type,  $\Delta$ Lhca1, and  $\Delta$ Lhca4 the red-most emission band is unchanged following excitation

at either wavelength. In the case of nonblocked energy transfer, thermal equilibrium between the emitting states is reached, leading to a common emission spectrum regardless of excitation wavelengths. However, if excitation energy cannot flow freely, local maxima of the emitting states will start to contribute, leading to changes in the shape and amplitude of spectra obtained under different excitation wavelengths.

Taken together, the above findings show that chlorophylls absorbing at 655, 665, and 688 nm belong to the linker chlorophylls preferentially associated with Lhca2 and/or Lhca3, while chlorophylls absorbing at 696 nm are linker chlorophylls associated with all Lhca proteins. The lack of Lhca2 or Lhca3 proteins and the linker pigments leads to imperfect energy transfer between the PSI core and LHCI, which, together with loss of the 712 nm-absorbing form, results in a blue shift of the red-most emission band. However, the absorption properties of the individual Lhca proteins are largely consistent with those observed for *in vitro* reconstituted systems (45; J. Ihalainen and R. Croce, unpublished results), in particular with regard to the 643 and 674 nm absorption bands in Lhca1 and/or Lhca4 and the 650 nm absorption band in Lhca2 and/or Lhca3. In addition, the results show that the red chlorophylls, at least in Lhca3 and Lhca2, are considerably red shifted in the native PSI–LHCI complex compared to those in the reconstituted systems.

## DISCUSSION

Our data obtained from antenna size measurements and pigment analysis of PSI complexes prepared from a set of *Arabidopsis* plants that are deficient in specific Lhca proteins, and hence differ in their PSI antenna protein composition, appear to agree, in principle, with the PSI–LHCI model recently published (24). The determined antenna sizes are consistent with the finding that higher plant LHCI is typically composed of four Lhca proteins *in vivo*. On the basis of the number and location of chlorophylls assigned to the structure there is little or no evidence for an additional two to four Lhca proteins. Any higher Chl/P700 ratios reported (64) can therefore probably be attributed to additional LHCIII attached to PSI. Our data do not confirm the suggestion (24, 65) that Lhca1 serves as an anchor for the whole LHCI as the protein patterns determined in this study show that the loss of Lhca1 has little impact on antenna size and Lhca protein composition. As the loss of Lhca4 clearly destabilizes the whole LHCI and leads to the greatest diminishment of LHCI antennae, we rather propose a central function for Lhca4 in LHCI association with PSI.

It must, however, be pointed out that LHCI is probably a rather flexible structure. Plants grown at different light intensities can differ in their amounts of individual Lhca proteins (34), PSI in different thylakoid compartments may also differ in Lhca protein content (30), and plants lacking LHCIII compensate by making more Lhca4 (66). It is likely that the structure in which one copy each of the Lhca1, Lhca2, Lhca3 and Lhca4 proteins is associated with PSI might be the “basic” and most abundant structure, which is stable enough to be prepared using standard PSI preparation protocols. In PSI preparations from wild-type plants the association of Lhca5 is weaker than in preparations from

$\Delta$ Lhca4 plants, and therefore this protein is presumably not recovered by the procedure used to prepare the complexes crystallized (67). Therefore, PSI–LHCI complexes with other polypeptide compositions exist *in vivo* and will probably accumulate only under certain conditions. We have as yet no clear evidence on the binding sites of the “additional” Lhca subunits, which perhaps could be added outside the basic structure. For Lhca5, for example, a clear interaction with Lhca2 is shown by the Lhca protein pattern as Lhca5 abundance is decreased when Lhca2 is absent (Figure 1B). A second possibility is that the positions may not be absolutely fixed, so that different polypeptides may occupy the same position. This might also be illustrated by the case of Lhca5, which strongly binds to the PSI preparations from the  $\Delta$ Lhca4 plants that lack all other Lhca proteins, including Lhca2, which seems to be involved in Lhca5–PSI interactions in the wild type. On the other hand, we believe that posttranslational events most likely decrease the stability of proteins lacking their normal “partners” in the structure, and this is more consistent with Lhca proteins, and all subunits, having fixed positions. If the system was very flexible, any partner could potentially stabilize any other protein. With respect to these considerations, the unusual binding pattern of Lhca5 seems to be an exception. It is clear that further studies are needed to fully understand the full complexity of the native LHCI structure, but in comparison to the PSI model for the wild type we can use the pigment quantifications and spectroscopic studies of the PSI particles from our Lhca-deficient lines to draw conclusions about the pigments associated with the individual LHCI subunits.

Of the 167 chlorophylls resolved in the structure (24) 101 are associated with the PSI core: 93 of which are also found in the cyanobacterial PSI and 8 are unique to higher plants. An additional 10 chlorophylls are located in the core, but at the peripheral binding site where the Lhca proteins assemble. It is not clear how these chlorophylls are affected when individual Lhca proteins are missing, and thus we have assumed an average number of chlorophylls is affected by the absence of each protein. It is worth to note that the PSI–LHCI holocomplex probably contains eight additional chlorophylls that could not be unambiguously assigned in the structure and which are most likely located in the PSI core (N. Nelson, personal communication). Within LHCI a total of 56 chlorophylls are located, 47 of which are coordinated by the four Lhca proteins and 9 are placed at the contact sites between the Lhca proteins. This indicates that four monomers of Lhca proteins might bind 47–56 chlorophyll molecules in total, exceeding the number of 6–10 chlorophylls per monomer determined by *in vitro* reconstitution studies (43, 44, 52, 60, 61). However, since there is consistency with the data reported for reconstituted and isolated native Lhca proteins, it is obvious that substantial proportions of the pigments bound in the native LHCI are lost during the preparation of monomers and do not bind in current reconstitution procedures.

On the basis of the data available so far, we use a model for the higher plant PSI–LHCI holocomplex in which the locations of the individual PSI polypeptides are based on cross-linking studies (42) and analyses of plants deficient in PSI subunits (for example, refs 51 and 68) and Lhca proteins (35, 54) as well as the crystal structure (24). In this model, we have attempted to pinpoint the locations of some of the

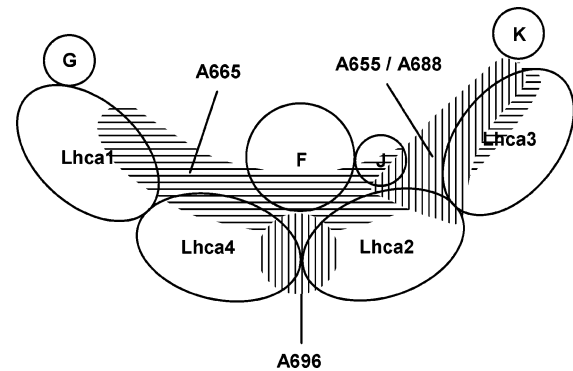


FIGURE 5: Assignment of chlorophyll absorption forms. Model of the PSI–LHCI interaction site with suggested locations of chlorophyll forms absorbing at indicated wavelengths (see text for details).

pigments that can be observed with different spectroscopic techniques. On the basis of the results from the absorbance difference spectra reported here (Figure 3), we were able to assign four of the absorption bands to chlorophylls located within the Lhca proteins and the PSI–LHCI interaction site (Figure 5). Since chlorophylls located between single Lhca polypeptides or between LHCI and the core will probably be lost during LHCI preparation, differences between the LHCI absorbance spectrum and the difference spectra in Figure 3 are likely to reflect such linker chlorophylls. We found a number of chlorophylls with absorption bands at 655, 665, 688, and 696 nm, which were not present in the LHCI preparation. The chlorophylls absorbing at 655 and 688 nm seemed to be mainly associated with Lhca2 and Lhca3, and since 688 nm forms are sometimes seen in isolated core particles (69), some pigments absorbing at 688 nm might be located near the core complex, but on the Lhca2/3 side. Chlorophylls absorbing at 665 and 696 nm were found to be associated with all Lhca proteins, making it difficult to pinpoint their exact locations. However, since the 696 nm form is most prominent in  $\Delta$ Lhca2,  $\Delta$ Lhca3, and  $\Delta$ Lhca4 plants and least prominent in the  $\Delta$ Lhca1 plants, this band may originate from the linker chlorophylls situated between Lhca4 and Lhca2. At about 696 nm a CD signal has been observed in the case of PSI–LHCI particles, which is lacking in isolated PSI core or LHCI spectra, indicating that this absorption band has an excitonic character involving chlorophylls located on both Lhca2 and Lhca4 (J. Ihalaenen, unpublished results). On the basis of absorbance analyses of reconstituted systems (43, 45; J. Ihalaenen and R. Croce, unpublished data), we assigned the pigments absorbing at 643, 650, and 674 nm to chlorophyll molecules associated with Lhca1, Lhca2/Lhca3, and Lhca4, respectively. It is evident that, as well as those associated with Lhca4, red chlorophylls are also present in the Lhca2–Lhca3 site of the complex. The chlorophylls responsible for the 712 nm absorption band are bound to Lhca3, whereas the red-most band of Lhca2 is located around 690 nm (45, 70). Taken together, we demonstrate a quite unique pattern of chlorophyll absorption forms *in vivo* for each of the Lhca monomers. On the other hand, larger scale patterns are also known, as red pigments are located on at least one Lhca protein of the Lhca1/Lhca4 and Lhca2/Lhca3 subcomplexes (Morosinotto et al., in preparation). A deeper understanding of the energy transfer processes within the light harvesting antenna of higher plant PSI also requires further in-depth

spectroscopic studies of the lines analyzed here and of knock-out plants that have been complemented by mutated versions of the Lhca proteins.

## REFERENCES

- Green, B. R., Pichersky, E., and Kloppstech, K. (1991) Chlorophyll *a/b*-binding proteins: an extended family, *Trends Biochem. Sci.* **16**, 181–186.
- Jansson, S. (1994) The light-harvesting chlorophyll *a/b*-binding proteins, *Biochim. Biophys. Acta* **1184**, 1–19.
- Jansson, S. (1999) A guide to the Lhc genes and their relatives in *Arabidopsis*, *Trends Plant Sci.* **4**, 236–240.
- Haldrup, A., Jensen, P. E., Lunde, C., and Scheller, H. V. (2001) Balance of power: a view of the mechanism of photosynthetic state transitions, *Trends Plant Sci.* **6**, 301–305.
- Kuehlbrandt, W., Wang, D. N., and Fujiyoshi, Y. (1994) Atomic model of plant light-harvesting complex by electron crystallography, *Nature* **367**, 614–621.
- Liu, Z., Yan, H., Wang, K., Kuang, T., Zhang, J., Gui, L., An, X., and Chang, W. (2004) Crystal structure of spinach major light-harvesting complex at 2.72 Å resolution, *Nature* **428**, 287–292.
- Zouni, A., Witt, H. T., Kern, J., Fromme, P., Krauss, N., Saenger, N., and Orth, P. (2001) Crystal structure of photosystem II from *Synechococcus elongatus* at 3.8 Å resolution, *Nature* **409**, 739–743.
- Ferreira, K. N., Iverson, T. M., Maghlaoui, K., Barber, J., and Iwata, S. (2004) Architecture of the photosynthetic oxygen-evolving center, *Science* **303**, 1831–1838.
- Boekema, E. J., van Roon, H., van Breemen, J. F. L., and Dekker, J. P. (1999) Supramolecular organization of photosystem II and its light-harvesting antenna in partially solubilized photosystem II membranes, *Eur. J. Biochem.* **266**, 444–452.
- Yakushevskaya, A. E., Keegstra, W., Boekema, E. J., Dekker, J. P., Andersson, J., Jansson, S., Ruban, A. V., and Horton, P. (2003) The structure of photosystem II in *Arabidopsis*: Localization of the CP26 and CP29 antenna complexes, *Biochemistry* **42**, 608–613.
- Krauss, N., Hinrichs, W., Witt, I., Fromme, P., Pritzkow, W., Dauter, Z., Betzel, C., Wilson, K. S., Witt, H. T., and Saenger, W. (1993) Three-dimensional structure of system I of photosynthesis at 6 Å resolution, *Nature* **361**, 326–330.
- Schubert, W.-D., Klukas, O., Krauss, N., Saenger, W., Fromme, P., and Witt, H. T. (1997) Photosystem I of *Synechococcus elongatus* at 4 Å resolution: comprehensive structure analysis, *J. Mol. Biol.* **272**, 741–769.
- Fromme, P., Jordan, P., and Krauss, N. (2001) Structure of Photosystem I, *Biochim. Biophys. Acta* **1507**, 5–31.
- Jordan, P., Fromme, P., Witt, H. T., Klukas, O., Saenger, W., and Krauss, N. (2001) Three-dimensional structure of cyanobacterial photosystem I at 2.5 Å resolution, *Nature* **411**, 909–917.
- Bibby, T. S., Nield, J., and Barber, J. (2001) Iron deficiency induces the formation of an antenna ring around trimeric photosystem I in cyanobacteria, *Nature* **412**, 743–745.
- Boekema, E. J., Hifney, A., Yakushevskaya, A. E., Piotrowski, M., Keegstra, W., Berry, S., Michel, K.-P., Pistorius, E. K., and Kruij, J. (2001a) A giant chlorophyll-protein complex induced by iron deficiency in cyanobacteria, *Nature* **412**, 745–748.
- Yeremenko, N., Kouril, R., Ihalainen, J. A., D'Haene, S., van Oosterwijk, N., Andrizhievskaya, E. G., Keegstra, W., Dekker, H. L., Hagemann, M., Boekema, E. J., Matthijs, H. C. P., and Dekker, J. P. (2004) Supramolecular organization and dual function of the IsiA chlorophyll-binding protein in cyanobacteria, *Biochemistry* **43**, 10308–10313.
- Melkozernov, A. N., Bibby, T. S., Lin, S., Barber, J., and Blankenship, R. E. (2003) Time-resolved absorption and emission show that the CP43' antenna ring of iron-stressed *Synechocystis* sp. PCC6803 is efficiently coupled to the photosystem I reaction center core, *Biochemistry* **42**, 3893–903.
- Andrizhievskaya, E. G., Frolow, D., van Grondelle, R., and Dekker, J. P. (2004) Energy transfer and trapping in the photosystem I complex of *Synechococcus* PCC 7942 and its supercomplex with IsiA, *Biochim. Biophys. Acta* **1656**, 104–113.
- Stauber, E. J., Fink, A., Markert, C., Kruse, O., Johanningmeier, U., and Hippler, M. (2003) Proteomics of *Chlamydomonas reinhardtii* light-harvesting proteins, *Eucaryotic Cell* **2**, 978–994.
- Tokutsu, R., Teramoto, H., Takahashi, Y., Ono, T., and Mingawa, J. (2004) The light-harvesting complex of photosystem I in *Chlamydomonas reinhardtii*: protein composition, gene structures and phylogenetic implications, *Plant Cell Physiol.* **45**, 138–145.
- Germano, M., Yakushevskaya, A. E., Keegstra, W., van Gorkom, H. J., Dekker, J. P., and Boekema, E. J. (2002) Supramolecular organization of photosystem I and light-harvesting complex I in *Chlamydomonas reinhardtii*, *FEBS Lett.* **525**, 121–125.
- Kargul, J., Nield, J., and Barber, J. (2003) Three-dimensional reconstruction of a light-harvesting complex I-photosystem I (LHCI-PSI) supercomplex from the green alga *Chlamydomonas reinhardtii*, *J. Biol. Chem.* **278**, 16135–16141.
- Ben-Shem, A., Frolow, F., and Nelson, N. (2003) Crystal structure of plant photosystem I, *Nature* **426**, 630–635.
- Mullet, J. E., Burke, J. J., and Arntzen, C. J. (1980) Chlorophyll proteins of photosystem I, *Plant Physiol.* **65**, 814–822.
- Bassi, R., and Simpson, D. (1987) Chlorophyll-protein complexes of barley photosystem I, *Eur. J. Biochem.* **163**, 221–230.
- Preiss, S., Peter, G. F., Anandan, S., and Thornber, P. (1993) The multiple pigment-proteins of the photosystem I antenna, *Photochem. Photobiol.* **57**, 152–157.
- Jensen, P. E., Rosgaard, L., Knoetzel, J., and Scheller, H. V. (2002) Photosystem I activity is increased in the absence of the PSI-G subunit, *J. Biol. Chem.* **277**, 2798–2803.
- Knoetzel, J., Svendsen, I., and Simpson, D. J. (1992) Identification of the photosystem I antenna polypeptides in barley, *Eur. J. Biochem.* **206**, 209–215.
- Jansson, S., Stefánsson, H., Nyström, U., Gustafsson, P., and Albertsson, P.-Å. (1997) Antenna protein composition of PS I and PS II in thylakoid subdomains, *Biochim. Biophys. Acta* **1320**, 297–309.
- Peter, G. F., Takeuchi, T., and Thornber, P. (1991) Solubilization and two-dimensional electrophoretic procedures for studying the organization and composition of photosynthetic membrane polypeptides, *Methods* **3**, 115–124.
- Bossmann, B., Knoetzel, J., and Jansson, S. (1997) Screening of *chlorina* mutants of barley (*Hordeum vulgare* L.) with antibodies against light-harvesting proteins of PS I and PS II: absence of specific antenna proteins, *Photosynth. Res.* **52**, 127–136.
- Zhang, H., Goodman, H. M., and Jansson, S. (1997) Antisense inhibition of the photosystem I antenna protein Lhca4 in *Arabidopsis thaliana*, *Plant Physiol.* **115**, 1525–1531.
- Bailey, S., Walters, R. G., Jansson, S., and Horton, P. (2001) Acclimation of *Arabidopsis thaliana* to the light environment: the existence of separate low light and high light responses, *Planta* **213**, 794–801.
- Ganeteg, U., Strand, Å., Gustafsson, P., and Jansson, S. (2001) The properties of the chlorophyll *a/b*-binding proteins Lhca2 and Lhca3 studied *in vivo* using antisense inhibition, *Plant Physiol.* **127**, 150–158.
- Ganeteg, U., Klimmek, F., and Jansson, S. (2004) Lhca5—an LHC-type protein associated with photosystem I, *Plant Mol. Biol.* **54**, 641–651.
- Storf, S., Stauber, E. J., Hippler, M., and Schmid, V. H. R. (2004) Proteomic analysis of the photosystem I light-harvesting antenna in tomato (*Lycopersicon esculentum*), *Biochemistry* **43**, 9214–9224.
- Gobets, B., van Stokkum, I. H. M., Rögner, M., Kruij, J., Schlodder, E., Karapetyan, N. V., Dekker, J. P., and van Grondelle, R. (2001) Time-resolved fluorescence emission measurements of photosystem I particles of various cyanobacteria: a unified compartmental model, *Biophys. J.* **81**, 407–424.
- Palsom, L. O., Flemming, C., Gobets, B., van Grondelle, R., Dekker, J. P., and Schlodder, E. (1998) Energy transfer and charge separation in photosystem I: P700 oxidation upon selective excitation of the long-wavelength antenna chlorophylls of *Synechococcus elongatus*, *Biophys. J.* **74**, 2611–2622.
- Lam, E., Ortiz, G., and Malkin, R. (1984) Chlorophyll *a/b* proteins of photosystem I, *FEBS Lett.* **168**, 10–14.
- Ihalainen, J. A., Gobets, B., Sznee, K., Brazzoli, M., Croce, R., Bassi, R., van Grondelle, R., Korppi-Tommola, J. E. I., and Dekker, J. P. (2000) Evidence for two spectroscopically different dimers of light-harvesting complex I from green plants, *Biochemistry* **39**, 8625–8631.
- Jansson, S., Andersen, B., and Scheller, H. V. (1996) Nearest-neighbor analysis of higher-plant photosystem I holocomplex, *Plant Physiol.* **112**, 409–420.
- Croce, R., Morosinotto, T., Castelletti, S., Breton, J., and Bassi, R. (2002) The Lhca antenna complexes of higher plants photosystem I, *Biochim. Biophys. Acta* **1556**, 29–40.

44. Schmid, V. H. R., Potthast, S., Wiener, M., Bergauer, V., Paulsen, H., and Storf, S. (2002) Pigment binding of photosystem I light-harvesting proteins, *J. Biol. Chem.* 277, 37307–37314.
45. Morosinotto, T., Breton, J., Bassi, R., and Croce, R. (2003) The nature of a chlorophyll ligand in Lhca proteins determines the far red fluorescence emission typical of photosystem I, *J. Biol. Chem.* 278, 49223–49229.
46. Storf, S., Klimmek, F., Jansson, S., and Schmid, V. H. R. (2004) Lhca5—a novel light-harvesting protein: pigment binding, spectral properties and oligomerization behavior, in *Photosynthesis: Fundamental Aspects to Global Perspectives* (van der Est, A., and Bruce, D., Eds.) Allen Press, Lawrence, KS (in press).
47. Boekema, E. J., Jensen, P. E., Schlodder, E., van Breemen, J. F. L., van Roon, H., Scheller, H. V., and Dekker, J. P. (2001) Green plant photosystem I binds light-harvesting complex I on one side of the complex, *Biochemistry* 40, 1029–1036.
48. Lunde, C., Jensen, P. E., Haldrup, A., Knoetzel, J., and Scheller, H. V. (2000) The PSI-H subunit of photosystem I is essential for state transitions in plant photosynthesis, *Nature* 408, 613–615.
49. Lunde, C., Jensen, P. E., Rosgaard, L., Haldrup, A., Gilpin, M. J., and Scheller, H. V. (2003) Plants impaired in state transitions can to a large degree compensate for their defect, *Plant Cell Physiol.* 44, 44–45.
50. Jensen, P. E., Haldrup, A., Zhang, S., and Scheller, H. V. (2004) The PSI-O subunit of plant photosystem I is involved in balancing the excitation pressure between the two photosystems, *J. Biol. Chem.* 279, 24212–24217.
51. Scheller, H. V., Jensen, P. E., Haldrup, A., Lunde, C., and Knoetzel, J. (2001) Role of subunits in eukaryotic photosystem I, *Biochim. Biophys. Acta* 1507, 41–60.
52. Morosinotto, T., Castelletti, S., Breton, J., Bassi, R., and Croce, R. (2002) Mutation analysis of Lhca1 antenna complex, *J. Biol. Chem.* 277, 36253–36261.
53. Castelletti, S., Morosinotto, T., Robert, B., Caffari, S., Bassi, R., and Croce, R. (2003) Recombinant Lhca2 and Lhca3 subunits of the photosystem I antenna system, *Biochemistry* 42, 4226–4234.
54. Ganeteg, U., K ulheim, C., Andersson, J., and Jansson, S. (2004) Is each light-harvesting complex protein important for plant fitness?, *Plant Physiol.* 134, 502–509.
55. Alonso, J. M., Stepanova, A. N., Leisse, T. J., Kim, C. J., Chen, H., Shinn, P., Stevenson, D. K., Zimmerman, J., Barajas, P., Cheuk, R., Gadriab, C., Heller, C., Jeske, A., Koesema, E., Meyers, C. C., Parker, H., Prednis, L., Ansari, Y., Choy, N., Deen, H., Geralt, M., Hazari, N., Hom, E., Karnes, M., Mulholland, C., Ndubaku, R., Schmidt, I., Guzman, P., Aguilar-Henonin, L., Schmid, M., Weigel, D., Carter, D. E., Marchand, T., Risseeuw, E., Brogden, D., Zeko, A., Crosby, W. L., Berry, C. C., and Ecker, J. R. (2003) Genome-Wide Insertional Mutagenesis of *Arabidopsis thaliana*, *Science* 301, 653–657.
56. Haldrup, A., Naver, H., and Scheller, H. V. (1999) The interaction between plastocyanin and photosystem I is inefficient in transgenic *Arabidopsis* plants lacking the PSI–N subunit of photosystem I, *Plant J.* 17, 689–698.
57. Gilmore, A. N., and Yamamoto, H. Y. (1991) Resolution of lutein and zeaxanthin using a non-encapped, lightly carbon-loaded C-18 high-performance liquid-chromatographic column, *J. Chromatogr.* 543, 137–145.
58. Zhang, S., and Scheller, H. V. (2004) Light-harvesting complex II binds to several small subunits of photosystem I, *J. Biol. Chem.* 279, 3180–3187.
59. Schmid, V. H., Cammarata, K. V., Bruns, B. U., and Schmidt, G. W. (1997) *In vitro* reconstitution of the photosystem I light-harvesting complex LHCI-730: Heterodimerization is required for antenna pigment organization, *Proc. Natl. Acad. Sci. U.S.A.* 94, 7667–7672.
60. Rupprecht, J., Paulsen, H., and Schmid, V. H. R. (2000) Protein domains required for formation of stable monomeric Lhca1- and Lhca4-complexes, *Photosynth. Res.* 63, 217–224.
61. Schmid, V. H. R., Thome, P., Ruhle, W., Paulsen, H., K uhlbrandt, W., and Rogl, H. (2001) Chlorophyll b is involved in long-wavelength spectral properties of light-harvesting complexes LHC I and LHC II, *FEBS Lett.* 499, 27–31.
62. Gobets, B., van Amerongen, H., Monshouwer, R., Kruip, J., R ogner, M., van Grondelle, R., and Dekker, J. P. (1994) Polarized site-selected fluorescence spectroscopy of isolated Photosystem I particles, *Biochim. Biophys. Acta* 1188, 75–85.
63. Croce, R., Zucchelli, G., Garlaschi, F., and Jennings, R. (1998) A thermal broadening study of the antenna chlorophylls in PSI-200, LHCI, and PSI core, *Biochemistry* 37, 17355–17360.
64. Danielsson, R., Albertsson, P.  ., Mamedov, F., and Styring, S. (2004) Quantification of photosystem I and II in different parts of the thylakoid membrane from spinach, *Biochim. Biophys. Acta* 1608, 53–61.
65. Ben-Shem, A., Frolow, F., and Nelson, N. (2004) Evolution of photosystem I—from symmetry through pseudosymmetry to asymmetry, *FEBS Lett.* 564, 274–280.
66. Andersson, J., Wentworth, M., Walters, R. G., Howard, C., Ruban, A. V., Horton, P., and Jansson, S. (2003) Absence of the Lhcb1 and Lhcb2 proteins of the light-harvesting complex of photosystem II—effects on photosynthesis, grana stacking and fitness, *Plant J.* 35, 305–361.
67. Ben-Shem, A., Nelson, N., and Frolow, F. (2003) Crystallization and initial X-ray diffraction studies of higher plant photosystem I, *Acta Crystallogr. D* 59, 1824–1827.
68. Pesaresi, P., Varotto, C., Richly, E., Lessnick, A., Salamini, F., and Leister, D. (2003) Protein–protein and protein–function relationships in *Arabidopsis* photosystem I: cluster analysis of PSI polypeptide levels and photosynthetic parameters in PSI mutants, *J. Plant Physiol.* 160, 17–22.
69. Ihalainen, J. A., R atsep, M., Jensen, P. E., Scheller, H. V., Croce, R., Bassi, R., Korppi-Tommola, J. E. I., and Freiberg, A. (2003) Red spectral forms of chlorophylls in green plant PSI—a site-selective and high-pressure spectroscopy study, *J. Phys. Chem. B* 107, 9086–9093.
70. Croce, R., Morosinotto, T., Ihalainen, J. A., Chojnicka, A., Breton, J., Dekker, J. P., van Grondelle, R., and Bassi, R. (2004) Origin of the 701 nm fluorescence emission of the Lhca2 subunit of higher plant photosystem, *J. Biol. Chem.* 279, 48543–48549.

BI047873G